AN ALTERNATING EVOLUTION APPROXIMATION TO SYSTEMS OF HYPERBOLIC CONSERVATION LAWS

HAILIANG LIU

Abstract. In this paper we present an alternating evolution (AE) approximation

$$\partial_t u + \sum_{j=1}^{d} \partial_j f_j(v) = \frac{1}{\epsilon}(v-u), \quad \partial_t v + \sum_{j=1}^{d} \partial_j f(u) = \frac{1}{\epsilon}(u-v),$$

to systems of hyperbolic conservation laws

$$\partial_t U + \sum_{j=1}^{d} \partial_j f_j(U) = 0, \quad U(x,0) = U_0(x),$$

in arbitrary spatial dimension. We prove the convergence of the approximate solutions towards an entropy solution of scalar multi-D conservation laws, and the L^1 contraction property for the approximate solution is established as well. It is also shown that such an approximation is extremely accurate in the sense that if initial data is prepared such that $u_0 = v_0 = U_0$, then no method error is induced as time evolves, and the exact entropy solution is precisely captured. Furthermore, in the approximation system time evolution of one variable is associated with spatial redistribution in another variable. These features render such an approximation ideal to be used for construction of high resolution numerical schemes to solve hyperbolic conservation laws. The usual obstacles caused by jumps crossing computational cell interfaces are not felt when both u and v are sampled alternatively, and reconstructed independently. Herewith we discuss the designing principle for constructing AE schemes, with illustration of two preliminary schemes for systems of conservation laws in one dimension. Both l^∞ monotonicity and the TVD (Total Variational Diminishing) property are established for these schemes when applied to the scalar laws.

Contents

1. Introduction 2
2. Alternating Evolution Approximation 3
3. Convergence of the Approximation 6
4. Scheme Construction 9
4.1. Lax-Friedrichs Averaging 9
4.2. Alternate sampling 9
4.3. Higher order reconstruction 9
4.4. Illustration of two AE schemes 10
5. Stability of Numerical Schemes 12
6. Numerical results 14
7. Concluding remarks 17
Acknowledgments 17
References 17

Key words and phrases. Lax-Friedrich scheme, hyperbolic conservation laws, alternating evolution.

1. Introduction

Let $U : \mathbb{R}^d \times \mathbb{R}^+ \to \mathbb{R}^m$ be the admissible weak solution to the Cauchy problem of systems of hyperbolic conservation laws

$$\partial_t U + \sum_{j=1}^{d} \partial_j f_j(U) = 0, \tag{1.1}$$

$$U(x,0) = U_0(x), \tag{1.2}$$

where $f_j \in \mathbb{R}^m$ is a smooth vector function and $U_0 \in L^\infty(\mathbb{R}^d)$.

In this paper we propose to approximate this solution by a novel approximation system of the form

$$\partial_t u + \sum_{j=1}^{d} \partial_j f_j(v) = \frac{1}{\epsilon}(v-u), \tag{1.3}$$

$$\partial_t v + \sum_{j=1}^{d} \partial_j f(u) = \frac{1}{\epsilon}(u-v), \tag{1.4}$$

with the initial condition

$$u(x,0) = u_0(x), \quad v(x,0) = v_0(x), \quad x \in \mathbb{R}^d. \tag{1.5}$$

Here, $\epsilon > 0$ is a scale parameter of user's choice. To see the consistency of this approximation with the conservation law (1.1), we introduce two new variables

$$\phi := \frac{u+v}{2}, \quad \psi := \frac{u-v}{2}.$$

Hence (ϕ, ψ) satisfy the following system of balance laws

$$\partial_t \phi + \sum_{j=1}^{d} \partial_j \left(\frac{f_j(\phi+\psi) + f_j(\phi-\psi)}{2} \right) = 0, \tag{1.6}$$

$$\partial_t \psi + \sum_{j=1}^{d} \partial_j \left(\frac{f_j(\phi-\psi) - f_j(\phi+\psi)}{2} \right) = -\frac{4}{\epsilon}\psi. \tag{1.7}$$

The system (1.6) is in conservative form, uniformly in ϵ, and the stiff source term now appears only in (1.7). The ψ is thus forced to approach zero exponentially as $\epsilon \downarrow 0$, and as a consequence, (1.1) is found to be the limit of (1.6).

We propose this type of approximation with an intention to use it as a guiding paradigm in the construction of numerical schemes for hyperbolic conservation laws. The idea of alternating evolution may very well apply to other problems. Our approximation framework has a simple formulation even for general multi-D system of conservation laws and is easy for numerical implementation. The system also has some special features: (i) this is an extremely accurate approximation; for scalar conservation laws it is proven that this system captures the exact entropy solution for original conservation laws provided both u_0 and v_0 are chosen as U_0. In other words, once the initial states are in equilibrium, they will remain in equilibrium; (ii) the approximate solution is as regular as the entropy solution, no additional stability condition needs to be imposed to drive approximate states to the entropy solution of conservation laws; (iii) it is important to observe that in this novel approximation the flux in (1.3) depends only on v and the flux in (1.4) depends only on u, this way the usual handling of wave propagation across cell interfaces can be replaced by a simple alternating update. The local balance between u and v is realized by the choice of parameter ϵ. Hence it is very convenient to construct high resolution schemes by utilizing some well established reconstruction techniques in literature to alternating samples of u and v. It is from this feature that the approximation derives its name: **alternating evolution**.

The plan of this paper is as follows: In Section 2 we discuss some conservative schemes for hyperbolic conservation laws and interpret our alternating evolution approximation as a model equation of the scheme when distinguishing the solution value at one grid and values at its neighbors by u and v, respectively. Some features are illustrated by an explicit example, and convergence results for general multi-D scalar conservation laws are presented. Section 3 is devoted to proofs of convergence of the AE approximation. In particular we show that the system shares the most elegant properties of scalar conservation laws:

strong L^1-stability and L^∞-monotonicity, for both $u+v$ and $u-v$. The difference $u-v$ will remain zero if it does so initially, or is driven to zero exponentially. These guarantee that the alternating evolution system admits a unique uniformly bounded solution for any $\epsilon > 0$, and the sequence of solutions forms a compact subset of $C([0,T); L^1(\mathbb{R}^d))$, for any $T > 0$. Then we prove the convergence of the sequence u^ϵ and v^ϵ to the unique entropy solution U of hyperbolic conservation laws with initial data $U_0 = (u_0 + v_0)/2$. The entropy inequality is ensured by the presence of damping when deriving from the formulation of weak solutions of the system. In the limit, $\epsilon \downarrow 0$, we find the celebrated family of entropy-entropy flux of Krúzkov [14]. Section 4 shows how to use our approximate system to design several novel numerical schemes for system of conservation laws in one dimension. Some stability properties of these schemes are presented in Section 5. The present paper concentrates on properties of the alternating evolution approximation and deriving design principles for numerical schemes. A selected set of numerical tests is presented in Section 6 to illustrate both 2nd and 3rd order AE schemes.

To put this work in proper perspective, we now recall some basic references concerning approximation models of hyperbolic conservation laws. Convergence theory is quite mature for scalar conservation laws due to the L^1 contraction property [34], which is often respected by the approximate scheme. The method of vanishing viscosity has long been recognized as an effective way to capture physical relevant shocks. Krùzkov [14] established the convergence of this approximation and derived the well known L^1 contraction estimate with his characterization of weak solutions. The first kinetic formulation is due to [27, 16]; see also [2, 26, 24] for related investigations. Relaxation phenomena is important in continuum physics. The use of relaxation schemes to construct solutions to hyperbolic conservation laws was advocated in [12], see also [13, 24] for some other relaxation approximations. In particular, convergence and stability of relaxation schemes introduced in [12] have been well justified, see, e.g., [21, 17, 18, 20, 19].

In addition to these approximate models with a small scale parameter, there is voluminous literature on finite difference schemes for hyperbolic conservation laws, in which the mesh size serves as a scale parameter. The earliest upwind scheme was due to Courant, Isaacson and Rees in 1952 [3], but not in conservative form. The Lax-Friedrich (LxF) scheme proposed in 1954, [15], is conservative but not upwinding, and suffers excessive numerical diffusion. In 1959, Godunov [6] proposed to evolve piece-wise cell average of the solution by evaluating the flux at the cell interface, which takes care of the wave propagation through locally solving Riemann problems. Therefore, the Godunov scheme is both conservative and upwinding. Since then various extensions of these forerunner schemes have been developed to achieve high resolution still non-oscillatory schemes, see e.g. [33, 8, 10, 35, 9, 29, 25, 11, 22, 23].

Observe that when computing entropy solutions to hyperbolic conservation laws over a set of computation cells, one has to carefully handle jumps crossing interfaces. These jumps of conserved quantities are not necessarily of physical reality, but mainly induced from reconstruction operations onto finite dimensional trial spaces. The LxF scheme updates the numerical solution at one grid point by using previous values at neighboring points, so no handling of interface jump is needed. One noticeable feature of the LxF scheme is the evolution of alternating samples, which was probably noted before but does not seem to be appreciated or explored. This feature is the heart of our AE approximation, in which we build a communication mechanism of two samples u and v through a relaxation process adjusted by the scale parameter ϵ.

We remark that the NT scheme [25], as a second order extension of the LxF scheme, evolves a staggered average of the piece-wise reconstruction of the computed solution crossing the cell interface, thus no Riemann solution solver is needed. Recently Liu [23] generalizes the NT scheme by evolving two pieces of information over redundant overlapping cells, therefore allows easy formulation of semi-discrete schemes. It is noted that the first order scheme derived in [23] when re-scaling the mesh size is equivalent to the first order AE scheme presented in this work — a variant of the Lax-Fredrichs scheme. A class of further refined local schemes derived from the AE approximation is reported in [1].

2. Alternating Evolution Approximation

To motivate our proposed approximation, we start with finite difference schemes for 1-D scalar conservation laws

$$\partial_t U + \partial_x f(U) = 0. \tag{2.1}$$

Let the xt-plane be covered by a rectangular gird with mesh size Δx in $x-$direction and Δt in the $t-$direction. It would seem natural to replace (2.1) by the difference equation

$$u_j^{n+1} = u_j^n - \frac{\lambda}{2}\left[f(u_{j+1}^n) - f(u_{j-1}^n)\right],$$

where $\lambda = \Delta t/\Delta x$ and u_j^n approximates $U(j\Delta x, n\Delta t)$. But this is known to be inappropriate because of the high degree of instability of this scheme. Replacing u_j^n by the average of its two neighbors $u_{j\pm1}^n$ we encounter the celebrated LxF scheme

$$u_j^{n+1} = \frac{u_{j+1}^n + u_{j-1}^n}{2} - \frac{\lambda}{2}\left[f(u_{j+1}^n) - f(u_{j-1}^n)\right]. \tag{2.2}$$

An alternative form of this scheme may be written as

$$u_j^{n+1} = \frac{1}{2\Delta x}\int_{x_{j-1}}^{x_{j+1}} R\left(\frac{x-x_j}{\epsilon}; u_{j-1}^n, u_{j+1}^n\right) dx, \quad x_{j-1} \le x \le x_{j+1}, \tag{2.3}$$

where $R(\frac{x-x_j}{\epsilon}; a, b)$ is the Riemann solution of (2.1) with Riemann data $w(t = t_n) = a$ for $x < x_j$; b for $x > x_j$ [5]. One noticeable feature of this scheme is that information on grids $j+n = even$ is independent of that on grids $j+n = odd$. However, the LxF solver (2.2) suffers from excessive numerical dissipation. A less dissipative but still stable scheme may be generated by a convex combination of above two schemes

$$u_j^{n+1} = u_j^n + \theta\left[\frac{u_{j+1}^n + u_{j-1}^n}{2} - u_j^n\right] - \frac{\lambda}{2}\left[f(u_{j+1}^n) - f(u_{j-1}^n)\right], \quad 0 < \theta < 1. \tag{2.4}$$

It was shown in [17] that this scheme generates l^1 stable discrete shocks under the CFL condition

$$\lambda \sup|f'| \le \theta < 1.$$

A more general conservative scheme may be written as

$$\begin{aligned} u_j^{n+1} = u_j^n &- \frac{\lambda}{2}\left[f(u_{j+1}^n) - f(u_{j-1}^n)\right] \\ &+ \frac{1}{2}\left[Q_{j+1/2}^n(u_{j+1}^n - u_j^n) + Q_{j-1/2}^n(u_{j-1}^n - u_j^n)\right]. \end{aligned} \tag{2.5}$$

Here, $Q_{j\pm1/2}^n$ serves as the numerical viscosity conuterbalancing the effect from the numerical flux in the first bracket; see [32]. It was proved in [17] that this scheme satisfies the l^2 energy inequality

$$\|u^{n+1}\|^2 - \|u^n\|^2 + c_0\|\Delta u^n\|^2 \le 0,$$

provided

$$\lambda \sup_{(s-u_j^{n+1})(s-u_{j\pm1}^n)\le 0}\left|\frac{f(u_{j\pm1}^n) - f(s)}{u_{j\pm1}^n - s}\right| \le Q_{j\pm1/2}^n < 1. \tag{2.6}$$

We observe that in (2.5) the value of u at any grid point is associated with those values at its neighboring grids. Such an association may lead to instability unless a CFL-type condition such as (2.6) is enforced. Motivated by these connections we propose a new model system by distinguishing numerical solutions at even and odd girds. More precisely, we denote the solution at even (or odd) grid points as u and those at odd (or even) girds as v, and pass to the limit $\Delta x, \Delta t \to 0$ in (2.5), keeping the $Q-$related terms by bringing in a scale parameter $\epsilon \sim \Delta t$. These actions lead to a coupled system for both u and v

$$u_t + f(v)_x = \frac{1}{\epsilon}Q(u,v)(v-u), \tag{2.7}$$

$$v_t + f(u)_x = \frac{1}{\epsilon}Q(u,v)(u-v). \tag{2.8}$$

The CFL condition (2.6) then leads to a scale condition for ϵ

$$\epsilon \le \frac{\Delta x}{\sup|f'|}Q \le \frac{\Delta x}{\sup|f'|}, \tag{2.9}$$

where $0 < Q \le 1$ indicates the amount of numerical dissipation. Note that the dependence of Q/ϵ on both u and v reflects the local communication of solutions at one grid and those at its neighbors. Incorporating such a communication factor into the parameter ϵ, in multi-D setting, we have the following simple model system,

$$\partial_t u + \nabla_x \cdot f(v) = \frac{1}{\epsilon}(v-u), \quad x \in \mathbb{R}^d \tag{2.10}$$

$$\partial_t v + \nabla_x \cdot f(u) = \frac{1}{\epsilon}(u-v), \tag{2.11}$$

which is a compact form of (1.3)-(1.4) with $f = (f_1, \cdots .f_d) \in \mathbb{R}^d$.

The main feature of this approximation to the system of conservation laws (2.1) is its high accuracy. This feature may be vividly illustrated for the linear scalar conservation laws with constant speed a:

$$\partial_t U + a\partial_x U = 0, \quad U(x,0) = U_0(x), \tag{2.12}$$

with an explicit solution $U(x,t) = U_0(x-at)$. In such a case the AE approximation system becomes

$$\partial_t u + a\partial_x v = \frac{1}{\epsilon}(v-u), \quad \partial_t v + a\partial_x u = \frac{1}{\epsilon}(u-v).$$

Its exact solution can be written as

$$u = \frac{1}{2}u_0(x-at)(1+e^{-4t/\epsilon}) + \frac{1}{2}v_0(x-at)(1-e^{-4t/\epsilon}),$$
$$v = \frac{1}{2}u_0(x-at)(1-e^{-4t/\epsilon}) + \frac{1}{2}v_0(x-at)(1+e^{-4t/\epsilon}).$$

From this we see that

- if we choose $u_0 = v_0 = U_0$ initially, then $u = v = U_0(x-at)$ gives the exact solution for the linear advection equation (2.12);
- both u and v converge exponentially to the average of $u_0(x-at)$ and $v_0(x-at)$ as ϵ/t becomes small. In particular, the quantity $u+v$ is $(u_0+v_0)(x-at)$ independent of ϵ. This shows that the exact solution for conservation laws can still be precisely captured if $u_0 + v_0 = 2U_0$ is enforced initially.

These nice properties are shown to still hold for scalar conservation laws with general smooth flux function in arbitrary spatial dimension $\mathbb{R}^d$.

Theorem 2.1. *For any $(u_0, v_0) \in L^1(\mathbb{R}^d) \cap L^\infty(\mathbb{R}^d)$ and each fixed ϵ, (2.10)-(2.11) admits a unique weak solution (u^ϵ, v^ϵ) on $\mathbb{R}^d \times \mathbb{R}^+$ such that $(u,v) \in C([0,\infty); L^1(\mathbb{R}^d))$. Moreover, there exists a bounded measurable function $U(x,t)$ on $\mathbb{R}^d \times \mathbb{R}^+$ such that as $\epsilon \downarrow 0$*

$$u^\epsilon \to U(x,t), \quad u^\epsilon - v^\epsilon \to 0 \quad (x,t) \in \mathbb{R}^d \times \mathbb{R}^+.$$

Also U is the entropy solution of (1.1) with initial data $U_0(x) = \frac{1}{2}(u_0(x) + v_0(x))$ for $x \in \mathbb{R}^d$.

Corollary 2.1. *Let U be the entropy solution of the scalar conservation laws (1.1) with initial data $U_0 \in L^1(\mathbb{R}^d) \cap L^\infty(\mathbb{R}^d)$, and (u^ϵ, v^ϵ) be the weak solution subject to initial data with $(u_0, v_0) \in L^\infty(\mathbb{R}^d)$. Then it holds*

$$\|u^\epsilon - v^\epsilon\|_{L^1(\mathbb{R}^d)} \le \|u_0 - v_0\|_{L^1(\mathbb{R}^d)} e^{-4t/\epsilon}.$$

Furthermore,
(i)if $u_0 + v_0 = 2U_0$, then

$$\lim_{t/\epsilon \to \infty} \|u^\epsilon(\cdot,t) - U(\cdot,t)\|_{L^1(\mathbb{R}^d)} = \lim_{t/\epsilon \to \infty} \|v^\epsilon(\cdot,t) - U(\cdot,t)\|_{L^1(\mathbb{R}^d)} = 0.$$

(ii) if $u_0 = v_0 = U_0$, then

$$u^\epsilon(x,t) = v^\epsilon(x,t) = U(x,t)$$

almost everywhere in $\mathbb{R}^d \times \mathbb{R}^+$.

Remarks:
1. For system of hyperbolic conservation laws, L^1 contraction is not valid any more. Convergence of approximate solutions may be studied by possibly exploiting existence of convex positively invariant domains; we refer to [5] for convergence of approximate solutions given by the vanishing viscosity method, and [28] for convergence of approximate solutions given by the semi-linear relaxation.
2. Nevertheless, this corollary confirms the high accuracy of the AE approximation to hyperbolic conservation laws (1.1). The initial discrepancy $v_0 - u_0$, if there is any, will decay exponentially within a

short period of time. This lays the foundation for using this approximation as a tool in constructing high resolution numerical schemes for systems of hyperbolic conservation laws.

3. Convergence of the Approximation

This section is devoted to a convergence theory as $\epsilon \downarrow 0$, for solutions of (2.10)-(2.11), and the relation to entropy solutions of multi-dimensional scalar conservation laws, i.e., (1.1) with $m = 1$.

We shall study the reformulation of the problem

$$\partial_t \phi + \nabla_x \cdot \left(\frac{f(\phi+\psi) + f(\phi-\psi)}{2} \right) = 0, \quad x \in \mathbb{R}^d, \tag{3.1}$$

$$\partial_t \psi + \nabla_x \cdot \left(\frac{f(\phi-\psi) - f(\phi+\psi)}{2} \right) = -\frac{4}{\epsilon}\psi, \tag{3.2}$$

where (ϕ, ψ) are related to (u, v) by

$$\phi := \frac{u+v}{2}, \quad \psi := \frac{u-v}{2}.$$

The first equation is in conservative form, uniformly in ϵ, and the stiff source term now appears only in the second equation. Due to the damping in equation (3.2), one should expect that, as $\epsilon \downarrow 0$, ψ^ϵ decays to zero, in which case (3.1) reduces to (1.1) with $U = \phi$.

We now examine the Cauchy problem of (3.1)-(3.2), under assigned initial conditions

$$\phi(x, 0) = \phi_0(x), \quad \psi(x, 0) = \psi_0(x), \quad x \in \mathbb{R}^d \tag{3.3}$$

with

$$\phi_0(x) = \frac{1}{2}(u_0(x) + v_0(x)), \quad \psi_0(x) = \frac{1}{2}(u_0(x) - v_0(x)), \quad x \in \mathbb{R}^d.$$

Note that (3.1)-(3.2) is a 2×2 system of hyperbolic balance laws, the classical theory guarantees that whenever the initial data (ϕ_0, ψ_0) are in $C_0^1(\mathbb{R}^d)$, then there exists a unique classical solution $(\phi, \psi)(\cdot, t) \in C_0^1(\mathbb{R}^d)$ of (3.1)-(3.2), defined on a maximal interval $[0, T)$, with $0 < T \le \infty$. Furthermore, when $T < \infty$,

$$\|(\phi, \psi)(t)\|_{L^\infty(\mathbb{R}^d)} \to \infty \quad t \uparrow T. \tag{3.4}$$

Moreover, under a broader class of initial data (3.3), the global weak solution does exist and derives from the dissipative effect in equation (3.2). The techniques for verifying our assertions below are adapted from those developed for other regularized approximations to scalar conservation laws, see e.g., [4, Chapter VI].

Theorem 3.1. *For any $(\phi_0, \psi_0) \in L^1(\mathbb{R}^d) \cap L^\infty(\mathbb{R}^d)$, there exists a unique weak solution (ϕ, ψ) of (3.1)-(3.2) on $\mathbb{R}^d \times \mathbb{R}^+$ such that $(\phi, \psi) \in C([0, \infty); L^1(\mathbb{R}^d))$. If*

$$a \le \phi_0(x) \le b, \quad a \le \psi_0(x) \le b,$$

then

$$a \le \phi(x, t) \le b, \quad a e^{-4t/\epsilon} \le \psi(x, t) \le b e^{-4t/\epsilon}, \quad (x, t) \in \mathbb{R}^d \times \mathbb{R}^+. \tag{3.5}$$

Furthermore, if $(\bar\phi, \bar\psi)$ is another such solution, with initial data $(\bar\phi_0, \bar\psi_0) \in L^1(\mathbb{R}^d) \cap L^\infty(\mathbb{R}^d)$, then, for any $t \in [0, \infty)$,

$$\int_{\mathbb{R}^d} \left[[\phi - \bar\phi]^+ + [\psi - \bar\psi]^+ \right] dx \le \int_{\mathbb{R}^d} \left[[\phi_0 - \bar\phi_0]^+ + [\psi_0 - \bar\psi_0]^+ \right] dx, \tag{3.6}$$

$$\|\phi - \bar\phi\|_{L^1(\mathbb{R}^d)} + \|\psi - \bar\psi\|_{L^1(\mathbb{R}^d)} \le \|\phi_0 - \bar\phi_0\|_{L^1(\mathbb{R}^d)} + \|\psi_0 - \bar\psi_0\|_{L^1(\mathbb{R}^d)}. \tag{3.7}$$

In particular, if

$$\phi_0(x) \le \bar\phi_0(x), \quad \psi_0(x) \le \bar\psi_0(x), \quad x \in \mathbb{R}^d, \tag{3.8}$$

then

$$\phi(x, t) \le \bar\phi(x, t), \quad \psi(x, t) \le \bar\psi(x, t), \quad (x, t) \in \mathbb{R}^d \times \mathbb{R}^+. \tag{3.9}$$

Proof. We shall verify assertions only within the context of classical solutions, with C_0^1 initial data, since the L^1-contraction estimate (3.7) enables one to construct weak solutions with any initial data in $L^1(\mathbb{R}^d) \cap L^\infty(\mathbb{R}^d)$ as L^1 limits of sequences of classical solutions.

Let both (ϕ, ψ) and $(\bar\phi, \bar\psi)$ are classical solutions with $C_0^1(\mathbb{R}^d)$ initial data. For $\delta > 0$, we employ a regularized primitive of the Heaviside function

$$\eta_\delta(w) = \begin{cases} 0 & \text{for } -\infty < w \le 0 \\ \frac{w^2}{4\delta} & \text{for } 0 < w \le 2\delta \\ w - \delta & \text{for } 2\delta < w \le \infty. \end{cases}$$

It follows from the system (3.1)-(3.2) that

$$\begin{aligned} &\partial_t[\eta_\delta(\phi - \bar\phi) + \eta_\delta(\psi - \bar\psi)] + \nabla_x \cdot [\eta_\delta'(\phi - \bar\phi)F_+ + \eta_\delta'(\psi - \bar\psi)F_-] \\ &\quad = -\frac{4}{\epsilon}(\psi - \bar\psi)\eta_\delta'(\psi - \bar\psi) + \eta_\delta''(\phi - \bar\phi)F_+ \cdot \nabla_x(\phi - \bar\phi) + \eta_\delta''(\psi - \bar\psi)F_- \cdot \nabla_x(\psi - \bar\psi), \end{aligned} \tag{3.10}$$

where

$$F_\pm := \frac{1}{2}[\pm f(\phi + \psi) + f(\phi - \psi) \mp f(\bar\phi + \bar\psi) - f(\bar\phi - \bar\psi)] \in \mathbb{R}^d. \tag{3.11}$$

For fixed values of all involved solutions of any sign, the first term on the right hand has a non-positive limit as $\delta \downarrow 0$. We thus integrate (3.10) over $\mathbb{R}^d \times (s, t)$ for fixed $0 < s < t < \infty$ to obtain

$$\begin{aligned} &\left[\int_{\mathbb{R}^d} \eta_\delta(\phi - \bar\phi) + \eta_\delta(\psi - \bar\psi) dx\right](t) - \left[\int_{\mathbb{R}^d} \eta_\delta(\phi - \bar\phi) + \eta_\delta(\psi - \bar\psi) dx\right](s) \\ &\quad \le \int_s^t \int_{\mathbb{R}^d} [\eta_\delta''(\phi - \bar\phi)F_+ \cdot \nabla_x(\phi - \bar\phi) + \eta_\delta'(\psi - \bar\psi)F_- \cdot \nabla_x(\psi - \bar\psi)] dx d\tau. \end{aligned} \tag{3.12}$$

Notice that both $\eta_\delta''(\phi-\bar\phi)F_+$ and $\eta_\delta''(\psi-\bar\psi)F_-$ are bounded, uniformly for $\delta > 0$, and converges pointwise to zero as $\delta \downarrow 0$. Therefore, (3.12) and the Lebesgue dominated convergence theorem imply

$$\left[\int_{\mathbb{R}^d} \left[[\phi - \bar\phi]^+ + [\psi - \bar\psi]^+\right] dx\right](t) \le \left[\int_{\mathbb{R}^d} \left[[\phi - \bar\phi]^+ + [\psi - \bar\psi]^+\right] dx\right](s),$$

from which we deduce the asserted inequality (3.6) by letting $s \downarrow 0$.

When (3.8) holds, (3.9) follows immediately from the inequality (3.6). Notice that, for any constants a and b, $(a, ae^{-4t/\epsilon})$ and $(b, be^{-4t/\epsilon})$ are particular solutions of (3.1)-(3.2), therefore we obtain the uniform bounds (3.5). These bounds prevent the blow-up (3.4) from happening at finite time and thus the solution exists on $\mathbb{R}^d \times \mathbb{R}^+$.

Finally we reverse the roles of (ϕ, ψ) and $(\bar\phi, \bar\psi)$ in (3.6) and add the resulting inequality to (3.6) to obtain the L^1 contraction estimate (3.7). This completes the proof. ☐

Next we investigate the limiting behavior of $(\phi^\epsilon, \psi^\epsilon)$ as $\epsilon \downarrow 0$.

Note that the flux in (3.2) becomes zero when $\psi^\epsilon = 0$. We thus multiply $sgn(\psi^\epsilon)$ on both sides of (3.2) and integrate over $\mathbb{R}^d$ to obtain

$$\frac{d}{dt}\int_{\mathbb{R}^d} |\psi^\epsilon| dx \le -\frac{4}{\epsilon}\int_{\mathbb{R}^d} |\psi^\epsilon| dx,$$

which upon integration gives

$$\|\psi^\epsilon\|_{L^1(\mathbb{R}^d)} \le \|\psi_0\|_{L^1(\mathbb{R}^d)} e^{-4t/\epsilon}. \tag{3.13}$$

This inequality captures the mechanism that induces the ψ^ϵ to decay to zero.

Theorem 3.2. *Let $(\phi^\epsilon, \psi^\epsilon)$ be a family of solutions of (3.1)-(3.2), with $(\phi_0, \psi_0) \in [L^1(\mathbb{R}^d) \cap L^\infty(\mathbb{R}^d)]^2$. Then there exists a bounded measurable function $U(x, t)$ on $\mathbb{R}^d \times \mathbb{R}^+$ such that as $\epsilon \downarrow 0$*

$$\phi^\epsilon \to U(x, t), \quad \psi^\epsilon \to 0, \quad (x, t) \in \mathbb{R}^d \times \mathbb{R}^+.$$

Furthermore, U is the entropy solution of (1.1) with initial data $U_0(x) = \phi_0(x)$ for $x \in \mathbb{R}^d$.

Proof. For $(x,t) \in \mathbb{R}^d \times \mathbb{R}^+$, set

$$F^\epsilon = \frac{1}{2}[f(\phi^\epsilon + \psi^\epsilon) + f(\phi^\epsilon - \psi^\epsilon)] \in \mathbb{R}^d, \tag{3.14}$$

then the conservation law (3.1) becomes

$$\partial_t \phi^\epsilon + \nabla_x \cdot F^\epsilon(x,t) = 0. \tag{3.15}$$

For convergence, we first show it in $L^\infty(\mathbb{R}^d)$ weak* for all $t > 0$, and then use the L^1 contraction to upgrade weak convergence to strong convergence in $L^1(\mathbb{R}^d)$. Define a family of functions

$$\Phi^\epsilon[\chi](t) := \int_{\mathbb{R}^d} \chi(x)\phi^\epsilon(x,t)dx, \quad t > 0,$$

for any fixed test function $\chi \in C_0^\infty(\mathbb{R}^d)$. From (3.15) it follows that $\Phi^\epsilon[\chi]$'s are continuous differentiable with derivative

$$\frac{d}{dt}\Phi^\epsilon[\chi](t) = \int_{\mathbb{R}^d} \nabla_x \chi \cdot F^\epsilon(x,t)dx$$

bounded, uniformly in $\epsilon > 0$. Arzela's theorem implies that there exists a sequence $\{\epsilon_n\}$, with $\epsilon_n \downarrow 0$ as $n \to \infty$, such that $\{\Phi^{\epsilon_n}[\chi]\}$ converges for all $t > 0$. By Cantor's diagonal process we may select a subsequence of $\{\epsilon_n\}$, denoted again by ϵ_n, so that $\{\Phi^{\epsilon_n}[\chi]\}$ is convergent for any $\chi \in L^1(\mathbb{R}^d)$. Thus for each $t > 0$, there exists a bounded measurable function on $\mathbb{R}^d$, denoted by $U(\cdot,t)$, such that

$$\phi^{\epsilon_n} \to U(x,t) \quad n \to \infty \tag{3.16}$$

in $L^\infty(\mathbb{R})$ weak*.

Next we recall that the L^1 contraction estimate (3.7) deduces the L^1 equicontinuity for the family $(\phi^\epsilon, \psi^\epsilon)$.

Hence, the convergence in (3.16) holds also strongly in $L^1(\mathbb{R}^d)$. In particular,

$$\phi^{\epsilon_n} \to U(x,t), \quad n \to \infty \tag{3.17}$$

almost everywhere on $\mathbb{R}^d \times \mathbb{R}^+$. From (3.13) it follows that

$$\psi^{\epsilon_n} \to 0, \quad n \to \infty \tag{3.18}$$

almost everywhere on $\mathbb{R}^d \times \mathbb{R}^+$. This together with (3.17) when inserted into (3.14) yields

$$F^{\epsilon_n} \to f(U(x,t)), \quad n \to \infty,$$

almost everywhere on $\mathbb{R}^d \times \mathbb{R}^+$. This together with (3.14), (3.15) and (3.17) shows that U is a weak solution of (1.1) with $m = 1$.

Finally we show U is also an entropy solution in the sense of Kruzkov [14]. We fix any constant k and write (3.10) for two solutions $(\phi^{\epsilon_n}, \psi^{\epsilon_n})$ and $(k, Ke^{-4t/\epsilon_n})$ with K to be chosen. We apply the resulting relation by a smooth test function, $\sigma(x,t)$, with compact support on $\mathbb{R}^d \times [0,\infty)$ and let $\delta \downarrow 0$. Using again the non-positive limit of the first term of the right hand, we obtain

$$\begin{aligned} &\int_0^\infty \int_{\mathbb{R}^d} \partial_t \sigma \left[(\phi^{\epsilon_n} - k)^+ + (\psi^{\epsilon_n} - Ke^{-4t/\epsilon_n})^+\right] dxdt \\ &\int_0^\infty \int_{\mathbb{R}^d} \nabla_x \sigma \cdot \left[H(\phi^{\epsilon_n} - k)F_+ + H(\psi^{\epsilon_n} - Ke^{-4t/\epsilon_n})F_-\right] dxdt \\ &+ \int_{\mathbb{R}^d} \sigma(x,0)\left[(\phi_0 - k)^+ + (\psi_0 - K)^+\right] dx \geq 0. \end{aligned} \tag{3.19}$$

Letting $n \to \infty$ and using (3.17), (3.18) we have

$$F_+ \to f(U) - f(k), \quad F_- \to 0, \quad n \to \infty$$

almost everywhere on $\mathbb{R}^d \times \mathbb{R}^+$. Thus (3.19), with large enough K such that $\psi_0 < K$, yields

$$\begin{aligned} &\int_0^\infty \int_{\mathbb{R}^d} \partial_t \sigma (U-k)^+ dxdt + \int_0^\infty \int_{\mathbb{R}^d} \nabla_x \sigma H(U-k) \cdot (f(U) - f(k))dxdt \\ &+ \int_{\mathbb{R}^d} \sigma(x,0)(\phi_0 - k)^+ dx \geq 0. \end{aligned} \tag{3.20}$$

Reversing the roles played by k and ϕ^{ϵ_n} in the above derivation, and adding the resulting inequality to (3.20), we obtain

$$\int_0^\infty \int_{\mathbb{R}^d} \partial_t \sigma \eta(U;k) + \nabla_x \sigma \cdot q(U;k) dx dt + \int_{\mathbb{R}^d} \sigma(x,0)\eta(\phi_0,k)dx \geq 0,$$

where $\eta(U;k) = |U-k|$ and $q(U;k) = \mathrm{sgn}(U-k)(f(U)-f(k)) \in \mathbb{R}^d$, with arbitrary $k \in \mathbb{R}$, is the celebrated family of entropy-entropy flux pairs of Kruzkov [14]. This verifies that U is the entropy weak solution of (1.1), with initial data given by $U_0 = \phi_0$. Since the entropy solution U is unique, the convergence in (3.17) and (3.18) along particular sequence applies also along the whole family $\{\epsilon\}$, as $\epsilon \downarrow 0$. The proof is thus complete. □

4. Scheme Construction

In this section we construct several numerical schemes for the one-dimensional system of conservation laws

$$\partial_t U(x,t) + \partial_x f(U(x,t)) = 0, \quad (x,t) \in \mathbb{R} \times \mathbb{R}^+, \tag{4.1}$$

subject to initial data $U(x,0) = U_0(x)$. Let $\{x_j\}$ be a uniform partition of the domain in $\mathbb{R}$ with $\Delta x = x_{j+1} - x_j$ and $x_{j\pm1} = x_j \pm \Delta x$.

4.1. **Lax-Friedrichs Averaging.**

Let $\bar{u}(x)$ denote the sliding average over

$$I_x = \{\xi | \quad x - \Delta x \leq \xi \leq x + \Delta x\}.$$

Integration of the 1-D AE system (1.3)-(1.4) over I_x gives

$$\frac{d}{dt}\bar{u}(x,t) = -\frac{\bar{u}(x,t)}{\epsilon} + \frac{1}{\epsilon}L[v](x,t), \tag{4.2}$$

$$\frac{d}{dt}\bar{v}(x,t) = -\frac{\bar{v}(x,t)}{\epsilon} + \frac{1}{\epsilon}L[u](x,t), \tag{4.3}$$

where x serves as a moving parameter and

$$L[U](x,t) := \bar{U}(x,t) - \frac{\epsilon}{2\Delta x}\left[f(U(x+\Delta x,t)) - f(U(x-\Delta x,t))\right]. \tag{4.4}$$

Our numerical scheme will be constructed by sampling both formulations (4.2) and (4.3) over alternating grids for u and v, respectively, with proper approximation of $L[U]$ defined in (4.4).

4.2. **Alternate sampling.**

For example, if we sample (4.2) at x_{2j} and (4.3) at x_{2j+1}, respectively, then we have

$$\frac{d}{dt}u_{2j}(t) = \frac{1}{\epsilon}[-u_{2j}(t) + L_{2j}[v](t)], \tag{4.5}$$

$$\frac{d}{dt}v_{2j+1}(t) = \frac{1}{\epsilon}[-v_{2j+1}(t) + L_{2j+1}[u](t)]. \tag{4.6}$$

The high accuracy of the scheme is realized via two steps: (i) high-order reconstruction U from averages $U_k(t)$ and evaluation of $L[U](t)$ accordingly; (ii) higher-order approximation of the above ODE system.

4.3. **Higher order reconstruction.**

To initiate the algorithm, at $t = 0$, we employ the initial data:

$$u_0(x) = v_0(x) = U_0(x), \quad x \in \mathbb{R}.$$

The grid values are defined through the Lax-Friedrichs averaging

$$U_k^0 = \frac{1}{2\Delta x}\int_{I_k} U_0(\xi)d\xi, \quad k \in \mathbb{Z},$$

where $I_k := [x_{k-1}, x_{k+1}]$. Given grid values U_k^n, say $n = 0$, we assign them to u and v alternatively,

$$U_k^n = \begin{cases} u_k^n, & k = 2j, \\ v_k^n, & k = 2j+1, \end{cases}$$

and then reconstruct piecewise polynomials $p[U^n](x)$ over intervals $\{I_k\}$ for k even and odd, respectively, such that

$$U_k^n = \frac{1}{2\Delta x}\int_{I_k} p[U^n](x)dx, \quad k \in \mathbb{Z}. \tag{4.7}$$

This piecewise polynomial reconstruction is conservative, (4.7), and should also be accurate of desired order, and non-oscillatory [8, 9, 33, 25]. Second order schemes require a piecewise linear reconstruction. Third order schemes employ a piecewise quadratic approximation.

With such reconstructed $p[U^n]$, we proceed to evaluate $L[U^n]$ as follows:

(i) At any even node $k = 2j$, using piecewise polynomial $p[v^n]$ constructed over $[x_{2j}, x_{2j+2}]$ we obtain

$$L_{2j}[v^n] = \frac{1}{2\Delta x}\int_{I_{2j}} p[v^n](x)dx - \frac{\epsilon}{2\Delta x}\left[f(p[v^n]_{2j+1}) - f(p[v^n]_{2j-1})\right]. \tag{4.8}$$

(ii) At any odd node $k = 2j+1$, using piecewise polynomials $p[u^n](x)$ constructed over $[x_{2j-1}, x_{2j+1}]$ we obtain $L_{2j+1}[u^n]$ as

$$L_{2j+1}[u^n] = \frac{1}{2\Delta x}\int_{I_{2j+1}} p[u^n](x)dx - \frac{\epsilon}{2\Delta x}\left[f(p[u^n]_{2j+2}) - f(p[u^n]_{2j})\right]. \tag{4.9}$$

These procedures together with the Runge-Kutta time discretization of the system (4.5)-(4.6) enable us to design a new class of high-resolution schemes for hyperbolic conservation laws, called AE schemes.

4.4. **Illustration of two AE schemes.** To illustrate, a first and a second order scheme are presented and some stability properties are verified.

If our reconstructed polynomial is piecewise constant, then

$$\frac{1}{2\Delta x}\int_{I_{2j}} p[v^n](\xi)d\xi = \frac{v^n_{2j+1}+v^n_{2j-1}}{2}, \quad \frac{1}{2\Delta x}\int_{I_{2j+1}} p[u^{n+1}](\xi)d\xi = \frac{u^{n+1}_{2j+2}+u^{n+1}_{2j}}{2}.$$

We thus arrive at a first order AE scheme

$$u^{n+1}_{2j} = (1-\kappa)u^n_{2j} + \kappa\left[\frac{v^n_{2j+1}+v^n_{2j-1}}{2} - \frac{\epsilon}{2\Delta x}(f(v^n_{2j+1}) - f(v^n_{2j-1}))\right], \tag{4.10}$$

$$v^{n+1}_{2j+1} = (1-\kappa)v^n_{2j+1} + \kappa\left[\frac{u^n_{2j+2}+u^n_{2j}}{2} - \frac{\epsilon}{2\Delta x}(f(u^n_{2j+2}) - f(u^n_{2j}))\right], \tag{4.11}$$

where $\kappa := \frac{\Delta t}{\epsilon}$. Motivated by the consideration in §2 for scalar conservation laws, ϵ should be chosen such that

$$\frac{\epsilon}{\Delta x}\max \rho(f'(U(x,t))) < 1. \tag{4.12}$$

Here ρ denotes the largest eigenvalue of the Jacobian matrix $f'(U)$. The terms in two brackets in (4.10)-(4.11) give the same value as that obtained by the Lax-Friedrichs scheme with time step ϵ. Therefore, under the condition (4.12), the above scheme enjoys same stability properties as the Lax-Friedrichs scheme does, see §5 for further details.

Next we present a second order scheme. The piecewise linear reconstruction is of the form

$$p[U^n](x) = U^n_k + s^n_k(x - x_k), \quad x \in I_k,$$

which gives the desired averaging U^n_k over I_k for any choice of s_k. Second-order accuracy is guaranteed if the numerical derivative

$$s_k = \partial_x U(x = x_k, t) + O(\Delta x).$$

Moreover the desired non-oscillatory property requires that we choose s^n_k with certain limiters [9, 33]. For example, we take the ENO second order reconstruction, for k =even or odd,

$$s^n_k = \text{minabs}\left\{\frac{U^n_{k+2} - U^n_k}{2\Delta x}, \frac{U^n_k - U^n_{k-2}}{2\Delta x}\right\}, \tag{4.13}$$

where $\text{minabs}(a, b) = a$ if $|a| \le |b|$; b otherwise [29].

With these reconstructions we obtain

$$\frac{1}{2\Delta x}\int_{I_k} p[U^n](\xi)d\xi = \frac{U^n_{k-1}+U^n_{k+1}}{2} + \frac{\Delta x}{4}(s^n_{k-1} - s^n_{k+1}).$$

Thus at $t = t_n$

$$L_k[U^n] := \left[\frac{U^n_{k+1}+U^n_{k-1}}{2} + \frac{\Delta x}{4}(s^n_{k-1} - s^n_{k+1}) - \frac{\epsilon}{2\Delta x}(f(U^n_{k+1}) - f(U^n_{k-1}))\right]. \tag{4.14}$$

Using a second order Runge-Kutta discretization we obtain the following second order AE scheme

$$u^*_{2j} = (1-\kappa)u^n_{2j} + \kappa L_{2j}[v^n], \tag{4.15}$$

$$v^*_{2j+1} = (1-\kappa)v^n_{2j+1} + \kappa L_{2j+1}[u^n], \tag{4.16}$$

$$u^{n+1}_{2j} = \frac{1}{2}u^n_{2j} + \frac{1}{2}\left[(1-\kappa)u^*_{2j} + \kappa L_{2j}[v^*]\right], \tag{4.17}$$

$$v^{n+1}_{2j+1} = \frac{1}{2}v^n_{2j+1} + \frac{1}{2}\left[(1-\kappa)v^*_{2j+1} + \kappa L_{2j+1}[u^*]\right]. \tag{4.18}$$

This second order scheme is easy to implement. When applied to scalar conservation laws, both the l^∞ bound and the TV bound are still ensured under some further restrictions on the scale parameter ϵ and time step. Third or even higher order schemes can be easily formulated.

It is straightforward to show that the above two schemes preserve the following conservation property

$$\sum_{j\in\mathbb{Z}}(u^{n+1}_{2j} + v^{n+1}_{2j+1}) = \sum_{j\in\mathbb{Z}}(u^n_{2j} + v^n_{2j+1}), \quad \forall\, n \in \mathbb{N}, \tag{4.19}$$

which is necessary for capturing physically relevant shock waves.

Remarks:

1. The scale parameter ϵ, restricted by a CFL-like condition (4.12), serves to adjust the numerical dissipation. The restriction on time step Δt is indicated by $\kappa < 1$. This leaves a room for appropriately choosing κ to optimize the performance of the AE schemes.

2. There are other options for the choice of s_k. For example, the MUSCL reconstruction [33] with

$$s^n_k = \text{minmod}\left\{\frac{U^n_{k+2} - U^n_k}{2\Delta x}, \frac{U^n_k - U^n_{k-2}}{2\Delta x}\right\}, \tag{4.20}$$

where $\text{minmod}(a,b) = \frac{1}{2}(\text{sgn}(x) + \text{sgn}(y))\min\{|a|,|b|\}$. A better choice is

$$s^n_k = minmod\left\{\alpha\frac{U^n_{k+1} - U^n_k}{\Delta x}, \frac{U^n_{k+1} - U^n_{k-1}}{2\Delta x}, \alpha\frac{U^n_k - U^n_{k-1}}{\Delta x}\right\},$$

where $minmod(a,b,c) = \min\{a^+, b^+, c^+\} + \max\{a^-, b^-, c^-\}$ and $\alpha \in [1,2]$. The larger the α, the less dissipative the scheme [31].

Note that $L[U^n]$ in the first order scheme (4.10)-(4.11) is nothing but those predicated by the Lax-Friedrich scheme. Hence it may also be evaluated by

$$L_k[U^n] := \frac{1}{2\Delta x}\int_{I_k} w(x, (t_n+\epsilon)-, p_{k-1}[U^n], p_{k+1}[U^n])dx, \tag{4.21}$$

where w is the generalized Riemann solution of

$$\partial_t w + \partial_x f(w) = 0, \quad t_n \le t \le t_n + \epsilon, \tag{4.22}$$

$$w(x, t_n) = \begin{cases} p_{k-1}[U^n], & x_{k-1} \le x < x_k, \\ p_{k+1}[U^n], & x_k < x \le x_{k+1}. \end{cases} \tag{4.23}$$

An alternative form of $L_k[U^n]$ in (4.21) can be written as

$$L_k[U^n] = \frac{1}{2\Delta x}\int_{I_k} p[U^n]dx - \frac{1}{2\Delta x}\int_{t_n}^{t_n+\epsilon}\left[f(w(x_{k+1})) - f(w(x_{k-1}))\right](\tau)d\tau, \quad k = \text{even } or \text{ odd},$$

which provides a base for the design of higher order extensions of the Lax-Friedrichs scheme for evaluation of $L[U^n]$ [25]. For implementation, certain quadrature rules are needed to evaluate the time integral involved in the above formula.

The above schemes retain conservation and consistency. In order to ensure convergence of the scheme, total variation bounds need to be verified, which will be established in the next section.

5. Stability of Numerical Schemes

Let $U^n := \{u^n, v^n\}$ be a computed solution, we shall use the following notations.

$$TV(U^n) = \sum_{j\in\mathbb{Z}} |v^n_{2j+1} - u^n_{2j}| + \sum_{j\in\mathbb{Z}} |u^n_{2j} - v^n_{2j-1}|.$$

Also

$$|u^n|_\infty = \max_{k=\text{even}} |U^n_k|, \quad |v^n|_\infty = \max_{k=\text{odd}} |U^n_k|$$

and $|U^n|_\infty := \max\{|u^n|_\infty, |v^n|_\infty\}$. Same notations still apply when U^n is replaced by $L[U^n]$.

Theorem 5.1. *Let $U^n := \{u^n, v^n\}$ be computed from the first order AE scheme (4.10)-(4.11) for scalar conservation laws. If the scale condition $\kappa < 1$ and*

$$\mu \max |f'| \le 1, \quad \mu := \frac{\epsilon}{\Delta x} \tag{5.1}$$

hold, then

$$|U^{n+1}|_\infty \le |U^n|_\infty, \quad n \in \mathbb{N}.$$

Furthermore, if $\bar{U}^n$ is another solution computed from this same scheme, it holds

$$\sum_{|k|\le N} |U^n_k - \bar{U}^n_k|\Delta x \le \sum_{|k|\le N+n} |U^0_k - \bar{U}^0_k|\Delta x.$$

Proof. Notice that the scheme (4.10) can be rewritten as

$$u^{n+1}_{2j} = (1-\kappa)u^n_{2j} + \kappa u^{n+\epsilon}_{2j}, \tag{5.2}$$

where

$$u^{n+\epsilon}_{2j} := \left[\frac{v^n_{2j+1} + v^n_{2j-1}}{2} - \frac{\epsilon}{2\Delta x}(f(v^n_{2j+1}) - f(v^n_{2j-1}))\right].$$

Here $u^{n+\epsilon}_{2j}$ gives the result of Lax-Friedrichs' scheme when applied to grid values $\{v^n_{2j\pm1}\}$. Under the condition (5.1), it is known [30] that

$$\max_{j\in\mathbb{Z}} |u^{n+\epsilon}_{2j}| \le \max_{j\in\mathbb{Z}} |v^n_{2j+1}| = |v^n|_\infty.$$

This when inserted into (5.2) again gives

$$\max_{j\in\mathbb{Z}} |u^{n+1}_{2j}| \le (1-\kappa)\max_j |u^n_{2j}| + \kappa \max_j |v^n_{2j+1}| \le \max_k |U^n_k|.$$

Similarly, from (4.11) it follows that

$$\begin{aligned}\max_{j\in\mathbb{Z}} |v^{n+1}_{2j+1}| &\le (1-\kappa)\max_j |v^n_{2j+1}| + \kappa \max_j |v^{n+\epsilon}_{2j+1}| \\ &\le \max\{\max_j |v^n_{2j+1}|, \max_j |u^n_{2j}|\} \\ &= \max_k |U^n_k|.\end{aligned}$$

A combination of the above gives $|U^{n+1}| \le |U^n|$. The L^1 contraction property is respected by the Lax-Friedrichs scheme [30], and the schemes in (4.10) and (4.11) are just a convex combination of values computed by the Lax-Friedrichs scheme and the value at the same grid in previous time step. These together ensure the L^1-contraction property as asserted. The proof is complete. □

For the second order scheme, the slope limiter is typically chosen to ensure that the total variation does not increase under operation of reconstructions:

$$TV[p[u^n](x)] \le TV[u^n], \quad TV[p[v^n](x)] \le TV[v^n]. \tag{5.3}$$

Note that this property is indeed satisfied by those slope limiters presented in previous section.

Lemma 5.1. *Let the slope s_k be chosen as (4.13) such that the TVD requirement (5.3) holds. Assume that the following scale condition is satisfied*

$$\mu \max_k |f'(U_k)| \leq 1/2. \tag{5.4}$$

Then the higher-order prediction of $L[U^n]$, (4.14), is l^∞ monotone

$$|L[U^n]|_\infty \leq |U^n|_\infty. \tag{5.5}$$

Moreover, it is TVD.

$$TV(L[U^n]) \leq TV(U^n). \tag{5.6}$$

Proof. Rewrite the prediction (4.14) as

$$L_k[U^n] = \frac{1}{2}(U^n_{k+1} + U^n_{k-1}) - \frac{\mu}{2}(\tilde{f}_{k+1} - \tilde{f}_{k-1}), \tag{5.7}$$

where the modified flux reads

$$\tilde{f}_k = f(U^n_k) + \frac{\Delta x}{2\mu} s^n_k.$$

Set

$$\beta_k := \begin{cases} \mu \frac{\tilde{f}_{k+1} - \tilde{f}_{k-1}}{U^n_{k+1} - U^n_{k-1}} & if \quad U^n_{k+1} \neq U^n_{k-1}, \\ 0 & if \quad U^n_{k+1} = U^n_{k-1}. \end{cases}$$

Then we have

$$L_k[U^n] = \frac{1}{2}(1 - \beta_k)U^n_{k+1} + \frac{1}{2}(1 + \beta_k)U^n_{k-1}.$$

This relation ensures the l^∞ monotonicity (5.5) provided $|\beta_k| \leq 1$ for any k even or odd.

In fact using both (4.13) and (5.4) we do have

$$\begin{aligned} \beta_k &\leq \mu \frac{|f(U^n_{k+1}) - f(U^n_{k-1})|}{|U^n_{k+1} - U^n_{k-1}|} + \frac{\Delta x \max\{|s^n_{k+1}|, |s^n_{k-1}|\}}{2|U^n_{k+1} - U^n_{k-1}|} \\ &\leq \mu|f'| + \frac{1}{2} \leq 1. \end{aligned}$$

Next we evaluate $TV[L[U^n]]$. From (5.7) it follows

$$\begin{aligned} L_k[U^n] - L_{k-1}[U^n] &= \frac{1}{2}(U^n_{k+1} - U^n_k) + \frac{1}{2}(U^n_{k-1} - U^n_{k-2}) - \frac{\mu}{2}(\tilde{f}_{k+1} - \tilde{f}_k - \tilde{f}_{k-1} + \tilde{f}_{k-2}) \\ &= \frac{1}{2}(1 - \beta_{k+1/2})(U^n_{k+1} - U^n_k) + \frac{1}{2}(1 + \beta_{k-3/2})(U^n_{k-1} - U^n_{k-2}), \end{aligned}$$

with

$$\beta_{k+1/2} := \begin{cases} \mu \frac{\tilde{f}_{k+1} - \tilde{f}_k}{U^n_{k+1} - U^n_k} & if \quad U^n_{k+1} \neq U^n_k, \\ 0 & if \quad U^n_{k+1} = U^n_k \end{cases}$$

satisfying $|\beta_{k+1/2}| \leq 1$ as argued above for β_k. These together lead to the desired TVD property (5.6). The proof is thus complete. □

With this lemma in mind we turn to

Theorem 5.2. *Consider the second order scheme (4.15)-(4.18) with $L[U^n]$ defined in (4.14). Assume the slope limiter s_k is chosen as in (4.13), $\kappa < 1$, and ϵ satisfies the scale condition (5.4). Then the scheme satisfies*

$$|U^{n+1}|_\infty \leq |U^n|_\infty \tag{5.8}$$

and

$$TV(U^{n+1}) \leq TV(U^n). \tag{5.9}$$

Proof. The estimates (5.5) stated in Lemma 5.1, which when combined with the fact that U^* is a convex combination of U^n and $L[U^n]$, lead to the following l^∞ monotonicity property

$$|u^*| \leq |U^n|_\infty, \quad |v^*| \leq |U^n|_\infty.$$

Recall that $L[U^n]$ has been shown to satisfy (5.5). We thus have

$$|L_{2j}[v^*]| \leq |U^n|_\infty, \quad |L_{2j+1}[u^*]| \leq |U^n|_\infty.$$

Recall that

$$u_{2j}^{n+1} = \frac{1}{2}u_{2j}^n + \frac{1}{2}\left\{(1-\kappa)\, u_{2j}^* + \kappa L_{2j}[v^*]\right\}. \tag{5.10}$$

For $\kappa \in (0,1)$ this convex combination enables us to conclude $|u_{2j}^{n+1}| \le |U^n|$. The same bound also applies to v_{2j+1}^{n+1}.

We now show the TVD property (5.9). A combination of (4.17) and (4.18) leads to

$$TV(U^{n+1}) \le \frac{1}{2}TV(U^n) + \frac{1}{2}(1-\kappa)TV(U^*) + \frac{\kappa}{2}TV(L[U^*]). \tag{5.11}$$

Using (4.15) and (4.16) we have

$$TV(U^*) \le (1-\kappa)TV(U^n) + \kappa TV(L[U^n]),$$

which when combined with (5.6) leads to

$$TV(U^*) \le TV(U^n).$$

Using (5.6) again for U^* we have

$$TV(L[U^*]) \le TV(U^*).$$

These estimates inserted into (5.11) yield (5.9) as asserted. □

Remarks:

1. The properties (5.8) and (5.9), when the time step is chosen such that

$$\frac{\Delta t}{\Delta x} \cdot \max|f'(u_0)| \le \frac{1}{2},$$

give both l^∞ and the TVD bound

$$|U^n|_\infty \le |U_0|_\infty, \qquad TV(U^n) \le TV(U^0).$$

The solution bound depends only on whether the prediction $L[U^n]$ respects corresponding properties (5.5) and (5.6). This quantity, $L[U^n]$, is adopted as a high-order approximation of the $L[U](x,t)$. The established result shows that the alternating evolution still preserves the stability property if a SSP (strong stability-preserving) Runge-Kutta discretization [7] is adopted.

2. For any reconstructed piecewise polynomials $p[U^n]$ satisfying (5.3), the prediction $L[U^n]$ computed from (4.21) does preserve both the l^∞ monotonicity and the TVD property.

In fact, since $L[u^n]$ is defined in (4.21) as the averaging of the local generalized Riemann solution w, we have

$$TV(L[u^n]) \le TV(w(x,(t_n+\epsilon)-), p_{k-1}[v^n], p_{k+1}[v^n]).$$

Recall the TVD property of entropy solutions of scalar conservation laws we have

$$TV(L[u^n]) \le TV(w(x,t_n)) = TV(p[v^n]) \le TV(v^n).$$

The TV bound for $L[v^n]$ can be justified in a similar manner.

6. Numerical results

For the scalar problem we have proved stability properties of our AE scheme. Its extension to systems may proceed by a straightforward *component-wise* application of the scalar recipe. In this section, we provide a few selected numerical results to demonstrate the behavior of our AE schemes of both 2nd and 3rd order. The first order AE scheme is just a generalized Lax-Friedrich scheme.

Example 6.1. One dimensional linear advection equation:

$$\begin{aligned} u_t + u_x &= 0, \qquad x \in [0,2]. \\ u(x,0) &= 1 + \sin \pi x, \quad u(0,t) = u(2\pi, t). \end{aligned}$$

For the given smooth initial condition, the exact solution is given by $u(x,t) = 1 + \sin \pi(x-t)$. In order to check the numerical accuracy, we take the final time $T = 2$. CFL number used is 0.95 and $\Delta t = 0.95\epsilon$ for both the second and third order schemes. The numerical accuracy is given in tables 1 and 2. The numerical accuracy test for smooth regions is carried out without the use of limiters.

Table 1: Errors and numerical accuracy for Example 6.1; $u_t + u_x = 0,\ x \in [0, 2],\ T = 2$, 2**nd order** scheme.

N	L^1 error	L^1 order	L^∞ error	L^∞ order
20	3.6282E-02	-	2.651112E-02	-
40	7.1057E-03	2.44	5.368203E-03	2.39
80	1.6210E-03	2.17	1.248352E-03	2.14
160	3.8992E-04	2.07	3.032424E-04	2.06
320	9.6418E-05	2.02	7.535488E-05	2.02
640	2.3867E-05	2.02	1.874511E-05	2.01
1280	5.9721E-06	2.00	4.684753E-06	2.00
2560	1.4917E-06	2.00	1.170863E-06	2.00

Table 2: Errors and numerical accuracy for Example 6.1; $u_t + u_x = 0,\ x \in [0, 2],\ T = 2$, 3**rd order** scheme.

N	L^1 error	L^1 order	L^∞ error	L^∞ order
20	3.8815E-02	-	3.0929E-02	-
40	4.9860E-03	3.07	3.9678E-03	3.07
80	6.2706E-04	3.05	4.9976E-04	3.04
160	7.8533E-05	3.02	6.2404E-05	3.03
320	9.8199E-06	3.01	7.7918E-06	3.02
640	1.2278E-06	3.01	9.7235E-07	3.01
1280	1.5348E-07	3.00	1.2131E-07	3.01
2560	1.9185E-08	3.00	1.5141E-08	3.00

Example 6.2. One dimensional invicid Burgers' equation:

$$\begin{aligned} u_t + \left(\frac{u^2}{2}\right)_x &= 0, \qquad x \in [0, 2], \\ u(x, 0) &= 1 + \sin \pi x, \quad u(0, t) = u(2\pi, t). \end{aligned}$$

We plot the discontinuous solution for different values of CFL number. From Figure 1, we can see that the numerical dissipation increases as ϵ becomes smaller.

Example 6.3. One dimensional nonlinear Buckley-Leverett problem:

$$u_t + \left(\frac{4u^2}{4u^2 + (1-u)^2}\right)_x = 0, \qquad x \in [-1, 1]$$

The initial condition is given by

$$u(x, 0) = \begin{cases} 1 & x \in [-\frac{1}{2}, 0] \\ 0 & \text{otherwise} \end{cases}$$

The flux is nonlinear and we use this example to test the scheme when the initial data is discontinuous. In order to check the resolution of discontinuities, we take the final time $T = 0.4$ and $N = 160$. We choose $\epsilon = 0.2\Delta x$ and $\Delta t = 0.5\epsilon$. The numerical results for second and third order schemes are given in Fig. 2 and Fig. 3.

Example 6.4. The Euler system of equations has the form

$$\begin{pmatrix} \rho \\ \rho v \\ E \end{pmatrix}_t + \begin{pmatrix} \rho v \\ \rho v^2 + p \\ v(E + p) \end{pmatrix}_x = 0$$

where $p = (\gamma - 1)(E - \frac{1}{2}\rho v^2); \gamma = 1.4$. We test the Euler equation for the Woodward-Colella problem: Here, $x \in [0, 1]$ and

$$(\rho, \rho v, E)(0) = \begin{cases} (1, 0, 2500) & x \in [0, 0.1] \\ (1, 0, 0.025) & x \in [0.1, 0.9] \\ (1, 0, 250) & x \in [0.9, 1] \end{cases}$$

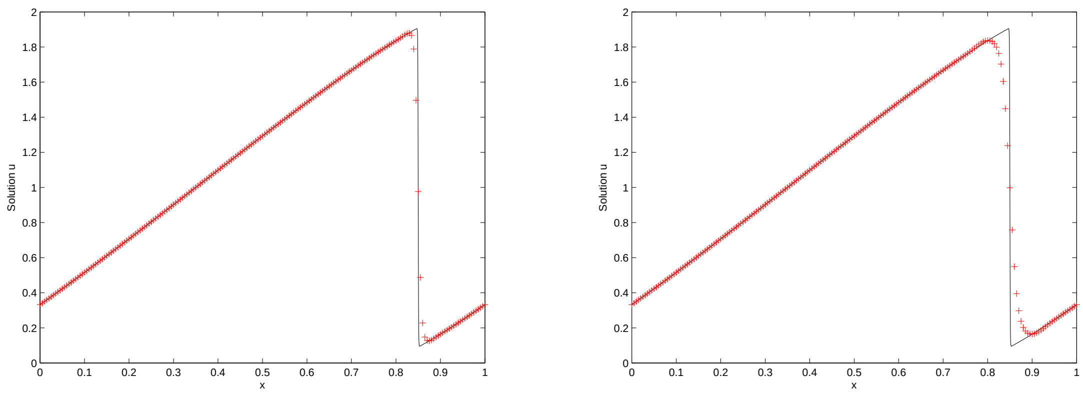

(a) $\epsilon = 0.1\Delta x$ and $\Delta t = 0.5\epsilon$.

(b) $\epsilon = 0.01\Delta x$ and $\Delta t = 0.5\epsilon$.

Figure 1: Plot for Burgers' equation at discontinuity on $[0, 2]$, $T = 0.7$, $N = 200$, 3**rd order** scheme to show the effect of change in ϵ.

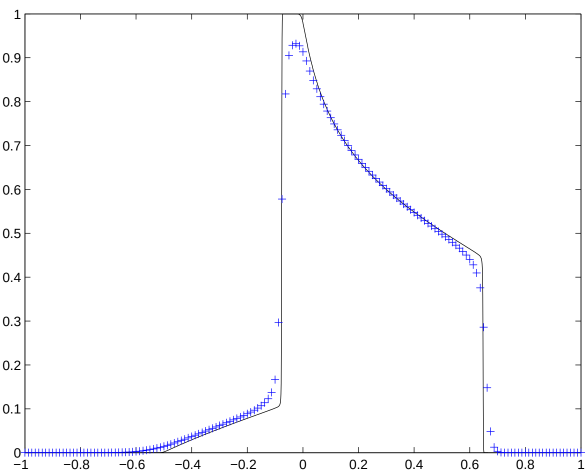

Figure 2: Plot for Buckley-Leverett problem 6.3 on $[-1, 1]$, $T = 0.4$, $N = 160$, $\epsilon = 0.2\Delta x$, $\Delta t = 0.5\epsilon$, 2**nd order** scheme.

The final time $T = 0.01, 0.03, 0.038$.

The Woodward-Colella problem involves the interaction of two blast waves. The initial data given presents one shock at $x = 0.1$ and the other at $x = 0.9$. The boundaries at $x = 0$ and $x = 1$ are solid walls with a reflective boundary condition. After a certain time, these two shocks collide with each other. At the final time step of $t = 0.038$, the flow field involves two shocks and three contact discontinuities. For numerical computations with Woodward Colella initial data, we choose $\epsilon = 0.01\Delta x$ and $\Delta t = 0.5\epsilon$. Fig. 4 shows the density profiles for both second and third order schemes for final time $T = 0.01, 0.03, 0.038$, respectively. The reference exact solution is calculated using 2560 grid points with $\epsilon = 0.01\Delta x$ and $\Delta t = 0.95\epsilon$.

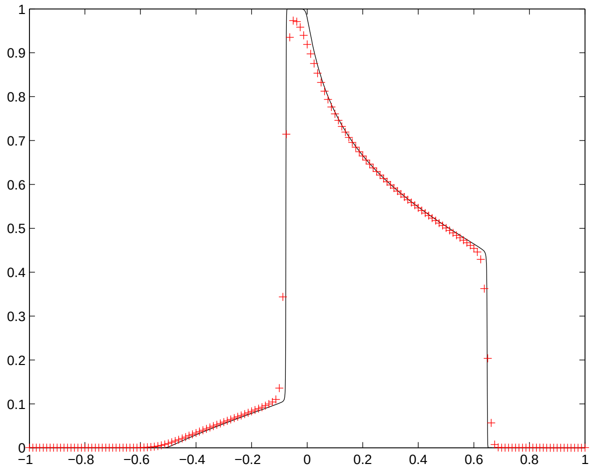

Figure 3: Plot for Buckley-Leverett problem 6.3 on $[-1, 1]$, $T = 0.4$, $N = 160$, $\epsilon = 0.2\Delta x$, $\Delta t = 0.5\epsilon$, **3rd order** scheme.

7. Concluding remarks

In this paper we have introduced a novel alternating evolution (AE) approximation to systems of hyperbolic conservation laws in arbitrary spatial dimension. For any fixed scale parameter ϵ, we show the global existence of weak solutions of this approximation, and further verify the convergence of approximate solutions towards an entropy solution of scalar conservation laws. In particular, if the initial data is chosen in such a way that two components u and v coincide, then the entropy solution is exactly captured by this AE approximation. This feature renders such an approximation ideal to be used for construction of high resolution numerical schemes to solve hyperbolic conservation laws. Some preliminary AE schemes are proposed and stability properties are established as well.

Beyond the preliminary schemes presented in this paper, further refined numerical schemes may be introduced by incorporating the local upwind information into the scheme through a proper choice of ϵ. Extensive numerical experiments and analysis of a class of local AE schemes are reported in [1].

We finally note that the idea of alternating evolution that was just applied to the hyperbolic conservation laws has a rich range of applicability. In future we shall generalize the AE approximation to a larger class of partial differential equations such as Hamilton-Jacobi equations and convection diffusion equations.

Acknowledgments

This research was supported by the National Science Foundation under Grant DMS05-05975. Haseena Ahmed did extensive numerical tests on a class of local AE schemes [1], as well as those presented in Section 6.

References

[1] H. Amhed and H. Liu. Implementation and analysis of a class of alternating evolution schemes for hyperbolic conservation laws. *preprint (2007).*

[2] Y. Brenier and L. Corrias. A kinetic formulation for multi-branch entropy solutions of scalar conservation laws. *Ann. Inst. H. Poincaré Anal. Non Linéaire*, 15(2):169–190, 1998.

[3] R. Courant, E. Isaacson, and M. Rees. On the solution of nonlinear hyperbolic differential equations by finite differences. *Comm. Pure. Appl. Math.*, 5:243–255, 1952.

[4] C. M. Dafermos. *Hyperbolic conservation laws in continuum physics*, volume 325 of *Grundlehren der Mathematischen Wissenschaften [Fundamental Principles of Mathematical Sciences].* Springer-Verlag, Berlin, second edition, 2005.

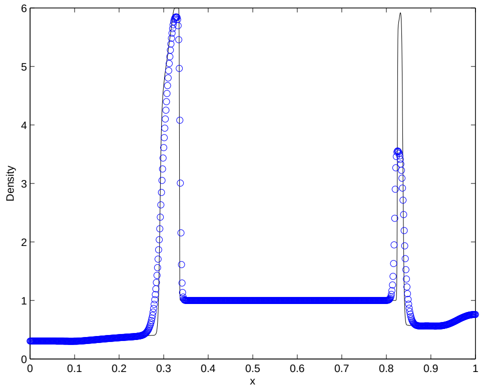

(a) Density with **2nd order** scheme.

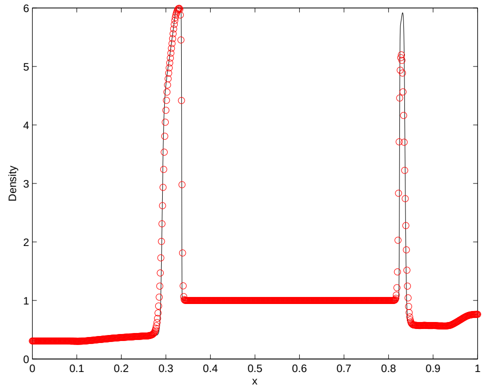

(b) Density with **3rd order** scheme.

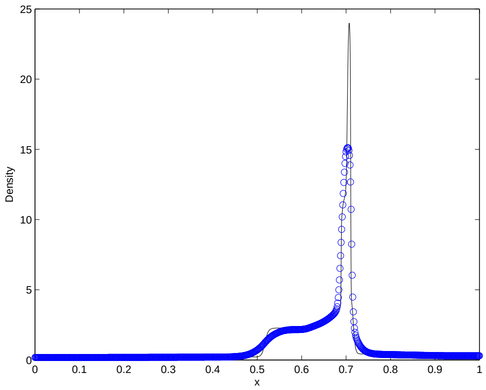

(c) Density with **2nd order** scheme.

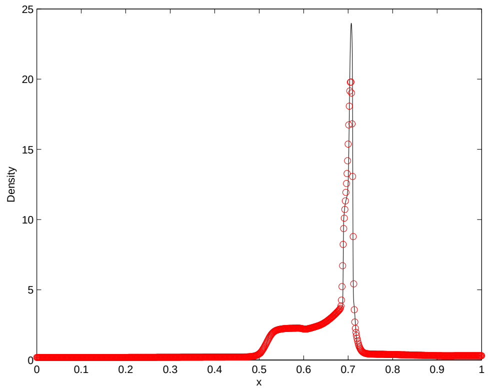

(d) Density with **3rd order** scheme.

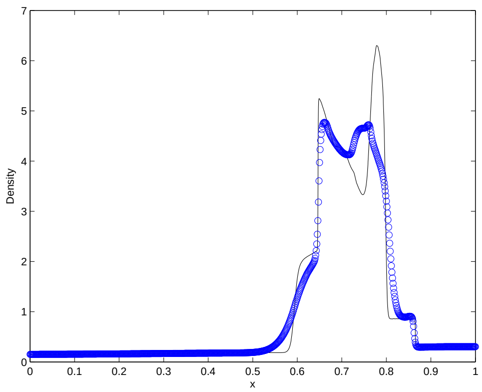

(e) Density with **2nd order** scheme.

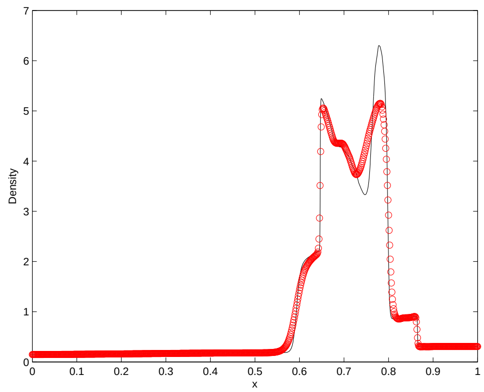

(f) Density with **3rd order** scheme.

Figure 4: Woodward and Colella Problem. Comparison of density profiles at $T = 0.01$(the 1st row), $T = 0.03$ (the 2nd row) and $T = 0.038$(the 3rd row). $N = 800$, $\epsilon = 0.01\Delta x$, $\Delta t = 0.5\epsilon$.

[5] R. J. DiPerna. Convergence of approximate solutions to conservation laws. *Arch. Rational Mech. Anal.*, 82(1):27–70, 1983.

[6] S. K. Godunov. A difference method for numerical calculation of discontinuous solutions of the equations of hydrodynamics. *Mat. Sb. (N.S.)*, 47 (89):271–306, 1959.

[7] S. Gottlieb, C.-W. Shu, and E. Tadmor. Strong stability-preserving high-order time discretization methods. *SIAM Rev.*, 43(1):89–112 (electronic), 2001.

[8] A. Harten. High resolution schemes for hyperbolic conservation laws. *J. Comput. Phys.*, 49(3):357–393, 1983.

[9] A. Harten, B. Engquist, S. Osher, and S. R. Chakravarthy. Uniformly high-order accurate essentially nonoscillatory schemes. III. *J. Comput. Phys.*, 71(2):231–303, 1987.

[10] A. Harten, P. D. Lax, and B. van Leer. On upstream differencing and Godunov-type schemes for hyperbolic conservation laws. *SIAM Rev.*, 25(1):35–61, 1983.

[11] G.-S. Jiang and C.-W. Shu. Efficient implementation of weighted ENO schemes. *J. Comput. Phys.*, 126(1):202–228, 1996.

[12] S. Jin and Z.-P. Xin. The relaxation schemes for systems of conservation laws in arbitrary space dimensions. *Comm. Pure Appl. Math.*, 48(3):235–276, 1995.

[13] M. A. Katsoulakis and A. E. Tzavaras. Contractive relaxation systems and the scalar multidimensional conservation law. *Comm. Partial Differential Equations*, 22(1-2):195–233, 1997.

[14] S. N. Kružkov. First order quasilinear equations with several independent variables. *Mat. Sb. (N.S.)*, 81 (123):228–255, 1970.

[15] P. D. Lax. Weak solutions of nonlinear hyperbolic equations and their numerical computation. *Comm. Pure Appl. Math.*, 7:159–193, 1954.

[16] P.-L. Lions, B. Perthame, and E. Tadmor. A kinetic formulation of multidimensional scalar conservation laws and related equations. *J. Amer. Math. Soc.*, 7(1):169–191, 1994.

[17] H. Liu. Asymptotic stability of relaxation shock profiles for hyperbolic conservation laws. *J. Differential Equations*, 192(2):285–307, 2003.

[18] H. Liu. Relaxation dynamics, scaling limits and convergence of relaxation schemes. In *Analysis and numerics for conservation laws*, pages 453–478. Springer, Berlin, 2005.

[19] H. Liu, J. Wang, and G. Warnecke. The lip$^+$-stability and error estimates for a relaxation scheme. *SIAM J. Numer. Anal.*, 38(4):1154–1170 (electronic), 2000.

[20] H. Liu and G. Warnecke. Convergence rates for relaxation schemes approximating conservation laws. *SIAM J. Numer. Anal.*, 37(4):1316–1337 (electronic), 2000.

[21] T.-P. Liu. Hyperbolic conservation laws with relaxation. *Comm. Math. Phys.*, 108(1):153–175, 1987.

[22] X.-D. Liu, S. Osher, and T. Chan. Weighted essentially non-oscillatory schemes. *J. Comput. Phys.*, 115(1):200–212, 1994.

[23] Y. Liu. Central schemes on overlapping cells. *J. Comput. Phys.*, 209(1):82–104, 2005.

[24] R. Natalini. A discrete kinetic approximation of entropy solutions to multidimensional scalar conservation laws. *J. Differential Equations*, 148(2):292–317, 1998.

[25] H. Nessyahu and E. Tadmor. Nonoscillatory central differencing for hyperbolic conservation laws. *J. Comput. Phys.*, 87(2):408–463, 1990.

[26] B. Perthame. Uniqueness and error estimates in first order quasilinear conservation laws via the kinetic entropy defect measure. *J. Math. Pures Appl. (9)*, 77(10):1055–1064, 1998.

[27] B. Perthame and E. Tadmor. A kinetic equation with kinetic entropy functions for scalar conservation laws. *Comm. Math. Phys.*, 136(3):501–517, 1991.

[28] D. Serre. Relaxations semi-linéaire et cinétique des systèmes de lois de conservation. *Ann. Inst. H. Poincaré Anal. Non Linéaire*, 17(2):169–192, 2000.

[29] C.-W. Shu and S. Osher. Efficient implementation of essentially nonoscillatory shock-capturing schemes. *J. Comput. Phys.*, 77(2):439–471, 1988.

[30] J. Smoller. *Shock waves and reaction-diffusion equations*, volume 258 of *Grundlehren der Mathematischen Wissenschaften [Fundamental Principles of Mathematical Sciences]*. Springer-Verlag, New York, second edition, 1994.

[31] P. K. Sweby. High resolution schemes using flux limiters for hyperbolic conservation laws. *SIAM J. Numer. Anal.*, 21(5):995–1011, 1984.

[32] E. Tadmor. Numerical viscosity and the entropy condition for conservative difference schemes. *Math. Comp.*, 43(168):369–381, 1984.

[33] B. van Leer. Towards the ultimate conservative difference scheme. V. A second-order sequel to Godunov's method [J. Comput. Phys. **32** (1979), no. 1, 101–136]. *J. Comput. Phys.*, 135(2):227–248, 1997. With an introduction by Ch. Hirsch, Commemoration of the 30th anniversary {of J. Comput. Phys.}.

[34] A. I. Vol′pert. Spaces BV and quasilinear equations. *Mat. Sb. (N.S.)*, 73 (115):255–302, 1967.

[35] P. Woodward and P. Colella. The numerical simulation of two-dimensional fluid flow with strong shocks. *J. Comput. Phys.*, 54(1):115–173, 1984.